

workup of procedure 12 should be carried out quickly, as 15 is subject to hydrolysis.

(16) $\text{Cp}^*\text{CpZr}(\text{CH}_3)_2$ (16). $\text{Cp}^*\text{CpZrCl}_3$ (13) (1 g, 2.76 mmol) was placed in a flask with 40 mL of Et_2O . A 1.9-mL portion of 3.0 M CH_3MgBr (5.7 mmol) in Et_2O was syringed into the flask at -78°C . The flask was warmed to 25°C and stirred for 6 h. The diethyl ether was removed, and 30 mL of petroleum ether was added. The resulting slurry was filtered and the MgBrCl washed five times with 10 mL of cold petroleum ether. Crystallization from petroleum ether afforded 790 mg of white 16 (89% yield). Anal. Calcd for $\text{C}_{17}\text{H}_{26}\text{Zr}$: C, 63.49; H, 8.15. Found: C, 63.64; H, 8.06.

(17) $\text{Cp}^*\text{Cp}^*\text{Zr}(\text{CH}_3)_2$ (17). Procedure 16 was followed except that 1 g of $\text{Cp}^*\text{Cp}^*\text{ZrCl}_2$ (14) (2.47 mmol) and 3.1 mL (5.5 mmol) of 1.8 M CH_3Li were used. Crystallization from petroleum ether afforded 690 mg of white 17 (76% yield). Anal. Calcd for $\text{C}_{20}\text{H}_{32}\text{Zr}$: C, 66.05; H, 8.87. Found: C, 66.01; H, 8.71.

(18) $(\text{MeInd})\text{Cp}^*\text{Zr}(\text{CH}_3)_2$ (18). Procedure 16 was followed except that 1 g of $(\text{MeInd})\text{Cp}^*\text{ZrCl}_2$ (15) (2.34 mmol) and 3 mL (5.4 mmol) of 1.8 M CH_3Li were combined. Upon removal of the petroleum ether, 790 mg of oily yellow 18 crystallized (87% yield).

(19) $(\text{Cp}^*\text{Cp}^*\text{ZrH}_2)_2$ (19). A 1.0-g sample of 13 in 20 mL of toluene was treated with 2.2 equiv of BuLi (1.6 M in hexane) at -80°C under H_2 (1 atm). The mixture was stirred and allowed to warm to room temperature. After 2 h toluene was removed in vacuo, and 20 mL of petroleum ether distilled in. After filtration

the solution was concentrated and cooled slowly to -80°C . The white crystals were filtered off at -80°C and washed with small portions of petroleum ether; yield 31%. Anal. Calcd for $\text{C}_{15}\text{H}_{22}\text{Zr}$: C, 61.37; H, 7.55. Found: C, 61.65; H, 7.40. Molecular weight (Bernhardt): 606; calculated for monomer, 294.

(20) $\text{Cp}^*\text{Cp}^*\text{ZrH}_2$ (20). To a stainless-steel Parr high-pressure apparatus, 500 mg of $\text{Cp}^*\text{Cp}^*\text{Zr}(\text{CH}_3)_2$ (17) (1.37 mmol) of 40 mL of toluene were added. H_2 (80 atm) was then introduced, and the reaction mixture was vigorously stirred for 24 h (final pressure 75 atm). The bomb was depressurized and opened. The yellow solution was then filtered, and the solvent was stripped. Petroleum ether was added, and 390 mg of pale yellow, microcrystalline 20 was collected on a frit (85% yield). Anal. Calcd for $\text{C}_{18}\text{H}_{28}\text{Zr}$: C, 64.41; H, 8.41. Found: C, 64.27; H, 8.32. Molecular weight (Bernhardt): 342; calculated for monomer, 336.

Acknowledgment. This work has been supported by the National Science Foundation (Grant No. CHE-8024869).

Registry No. 1, 75181-07-6; 2, 81476-62-2; 3, 81476-63-3; 4, 81476-64-4; 5, 81476-65-5; 6, 81476-66-6; 7, 81476-67-7; 8, 81476-68-8; 9, 81476-69-9; 10, 81476-70-2; 11, 81476-71-3; 12, 81476-72-4; 13, 81476-73-5; 14, 81476-74-6; 15, 81476-75-7; 16, 81476-76-8; 17, 81496-91-5; 18, 81476-77-9; 19, 81476-78-0; 20, 81496-92-6; ZrCl_4 , 10026-11-6; CH_3Br , 74-83-9; PhCH_2Cl , 100-44-7; PhBr , 108-86-1; 1-methylindene, 767-59-9; 1-indanone, 83-33-0.

Synthesis, Characterization, and Structures of Aluminum Pentamethylcyclopentadienyl Complexes, $[\eta^3-(\text{CH}_3)_5\text{C}_5\text{Al}(\text{Cl})\text{R}]_2$ ($\text{R} = \text{CH}_3, \text{C}_2\text{H}_5, i\text{-C}_4\text{H}_9$): Examples of η^3 -Cyclopentadienyl Ligand Coordination

P. R. Schonberg, R. T. Paine,*¹ C. F. Campana, and E. N. Duesler

Department of Chemistry, University of New Mexico, Albuquerque, New Mexico 87131

Received October 21, 1982

The reactions of $\text{Li}[(\text{CH}_3)_5\text{C}_5]$ and $[(\text{CH}_3)_5\text{C}_5]\text{MgCl}$ with the alkyl aluminum halides $[(\text{CH}_3)_2\text{AlCl}]_2$, $[(\text{C}_2\text{H}_5)_2\text{AlCl}]_2$, $[\text{C}_2\text{H}_5\text{AlCl}_2]_2$, $[(i\text{-C}_4\text{H}_9)_2\text{AlCl}]_2$, and $[(i\text{-C}_4\text{H}_9)\text{AlCl}_2]_2$ are reported. The new compounds $[(\text{CH}_3)_5\text{C}_5\text{Al}(\text{Cl})\text{R}]_2$ ($\text{R} = \text{CH}_3, \text{C}_2\text{H}_5$, and $i\text{-C}_4\text{H}_9$) have been isolated and characterized by mass, infrared, and ^1H and ^{13}C NMR spectroscopy. In addition, the complexes $[(\text{CH}_3)_5\text{C}_5\text{Al}(\text{Cl})(\text{CH}_3)]_2$ and $[(\text{CH}_3)_5\text{C}_5\text{Al}(\text{Cl})(i\text{-C}_4\text{H}_9)]_2$ have been subjected to single-crystal X-ray structural analysis. $[(\text{CH}_3)_5\text{C}_5\text{Al}(\text{Cl})(\text{CH}_3)]_2$ (1) crystallizes in the monoclinic space group $P2_1/c$ with $a = 8.550$ (2) Å, $b = 8.917$ (3) Å, $c = 16.012$ (7) Å, $\beta = 104.65$ (2)°, $Z = 2$, $V = 1181.1$ (7) Å³, and $\rho = 1.20$ g cm⁻³. Data were collected at -65°C by using Mo $K\alpha$ radiation, and full-matrix least-squares refinement converged with final discrepancy indices $R_F = 0.061$ and $R_{wF} = 0.092$. The complex $[(\text{CH}_3)_5\text{C}_5\text{Al}(\text{Cl})(i\text{-C}_4\text{H}_9)]_2$ (3) crystallizes in the monoclinic space group $P2_1/n$ with $a = 13.040$ (6) Å, $b = 8.928$ (2) Å, $c = 13.083$ (3) Å, $\beta = 98.06$ (3)°, $Z = 2$, $V = 1508.3$ (9) Å³, and $\rho = 1.12$ g cm⁻³. Data were collected at 27°C by using Mo $K\alpha$ radiation, and full-matrix least-squares refinement converged with final discrepancy indices $R_F = 0.075$ and $R_{wF} = 0.095$. The dimeric molecules possess C_i symmetry and nearly conform to C_{2h} - $2m$ symmetry. The structures reveal unusual planar, η^3 - $(\text{CH}_3)_5\text{C}_5$ ring attachments to the central Al_2Cl_2 units. In 1, the C_5 ring-Al interatomic distances are 2.100 (3), 2.252 (3), 2.282 (3), 2.499 (3), and 2.518 (3) Å. The last two distances are considered to be nonbonding distances. In 3, the related distances are 2.096 (9), 2.359 (8), 2.243 (8), 2.616 (9), and 2.563 (9) Å. Several structural parameters suggest greater nonbonded or steric repulsions in 3 compared to 1 which result in a distortion toward an η^2 configuration. Nonparameterized molecular orbital calculations have been used to help clarify the bonding mode observed in these compounds.

Introduction

The structural chemistry of cyclopentadienide and cyclopentadienyl complexes of the transition metals has been extensively studied,² and metal atom-Cp ring bonding is

well understood for the η^5 and η^1 coordination modes.³⁻⁵ On the other hand, relatively little attention has been given to the synthesis and structural characterization of met-

(1) To whom correspondence should be addressed.

(2) Haaland, A. *Acc. Chem. Res.* 1979, 12, 415 and references therein.

(3) Lauher, J. W.; Hoffmann, R. *J. Am. Chem. Soc.* 1976, 98, 1729.

(4) Anh, N. T.; Elian, M.; Hoffmann, R. *J. Am. Chem. Soc.* 1978, 100, 1110.

(5) Mingos, D. M. P. *Adv. Organomet. Chem.* 1976, 15, 1.

al-Cp compounds containing intermediate ring hapticities.⁶ Similarly, the structures and bonding in nonmetal cyclopentadienide compounds have been unevenly studied. The predominant hapticity, as indicated by spectroscopic data, is η^1 with examples provided by $B(C_2H_5)_2Cp$,⁷ H_3CCp ,⁸ $M(CH_3)_3Cp$ ($M = Si, Ge, Sn$),⁹ PF_2Cp ,^{10,11} and $AsCp_3$.¹² Each of these compounds is reported to undergo fluxional rearrangements (1,2 or 1,3 shifts) at 25 °C, and the dynamics of these motions have been studied by NMR techniques.¹³ A few reports of η^5 -Cp coordination in gaseous molecules containing metalloid elements $TiCp$,¹⁴ $InCp$,¹⁵ and $PbCp_2$ ¹⁶ have appeared, and several examples of solid-state structures containing bridging η^1 - or η^5 -Cp rings also exist.¹⁷ The occurrence of intermediate hapticities and "slipped" ring configurations in nonmetal or metalloid cyclopentadienide compounds, on the other hand, appears to be rare. Two examples of slipped ring configurations are provided by $CpSnCl$ ¹⁸ and $[(CH_3)_5C_5]_2Sn$.¹⁹

The interactions of aluminum atoms with olefins, and the Cp ligand in particular, are of interest in the structural context described above as well as with relation to the nature of carbalumination reactions.^{20,21} The isolation²² and spectroscopic detection²³ of several aluminum-olefin and aluminum-acetylene complexes provide some evidence for the operation of π bonding in carbalumination reaction transients. However, the σ - π bonding character in the interaction of aluminum atoms with cyclopentadienide has remained unclear. In 1961, Giannini and Cesca²⁴ reported

a reaction of $NaCp$ with $[Al(C_2H_5)_2Cl]_2$, and the proposed product $Al(C_2H_5)_2Cp$ was determined to be dimeric in benzene solution. Subsequent variable-temperature ¹H NMR studies by Kroll and Naegele²⁵ were used to assign a dynamic η^1 Cp-Al coordination geometry for a series of R_2AlCp compounds. Infrared spectroscopic analysis of solid- $(CH_3)_2AlCp$ by Haaland alternatively suggested a η^5 Al-Cp interaction;²⁶ however, electron diffraction analysis of gaseous $(CH_3)_2AlCp$ was found to be most consistent with an η^2 or η^3 configuration.²⁷ Molecular orbital calculations indicated that rotational barriers to exchange, $\eta^2 \leftrightarrow \eta^3 \leftrightarrow \eta^5$, should be low.²⁸ Lastly, Haaland and co-workers reported that vibrational spectra for R_2AlCp compounds in nonpolar solvents were more consistent with η^2 or η^3 structures.²⁹ These intriguing structural ambiguities and a general interest in the nature of aluminum-olefin compounds led us to investigate the interactions of aluminum alkyl fragments and cyclopentadienyl ligands.³⁰ We report here the syntheses and characterization of several new aluminum pentamethylcyclopentadienyl compounds, structure determinations of $[(CH_3)_5C_5]Al(C_2H_5)Cl_2$ and $[(CH_3)_5C_5]Al(i-C_4H_9)Cl_2$, and molecular orbital analysis for a simplified model compound $[(C_5H_5)Al(CH_3)Cl]_2$.

Experimental Section

General Information. Standard vacuum and inert atmosphere synthetic techniques were used for the manipulations of all reagents and products. Mass spectra were recorded on a Du Pont Model 21-491 spectrometer operating at 70 eV using a solids probe (source temperature 80 °C). Infrared spectra were recorded from KBr pellets with a Perkin-Elmer Model 621 spectrometer, and calibrations were accomplished by using polystyrene film absorptions. The NMR spectra were recorded on a Varian XL-100 NMR spectrometer operating at 25.2 MHz (¹³C) and 100 MHz (¹H). Some ¹H spectra also were recorded on Varian FT-80A and Varian EM-360 spectrometers. Samples for the XL-100 spectrometer were contained in 5-mm tubes rigidly held by Teflon spacers in a 12-mm tube containing a deuterated lock solvent. Samples for the FT-80 spectrometer were confined in 5-mm tubes containing an internal deuterated lock solvent. The spectra standard was $(CH_3)_4Si$ (¹³C, ¹H).

Materials. The alkyl aluminum halides were purchased from Ethyl Corp. and Ventron Corp. and they were used without further purification. Pentamethylcyclopentadiene was prepared by literature methods³¹ or purchased from Strem Chemicals Inc. *n*-Butyllithium was purchased from Aldrich Chemical Co. and isopropylmagnesium chloride was purchased from Ventron Corp. The solvents were rigorously dried by standard methods, stored over nitrogen, and vacuum distilled prior to the preparation of the reagent mixtures.

Pentamethylcyclopentadienide (Cp*) reagents were prepared immediately prior to the syntheses of the aluminum compounds. Solvent-free Cp*MgCl was obtained from the reaction of (*i*-Pr)MgCl with Cp*H in boiling toluene. The resulting orange slurry was used directly in the syntheses described below. Cp*Li was prepared by the reaction of *n*-butyllithium and Cp*H in THF, toluene, or hexane. The spongy white solid also was used directly in the syntheses of the aluminum compounds.

Preparation of $[Cp^*Al(CH_3)Cl]_2$, 1. Typically, 10 mmol of $[(CH_3)_2AlCl]_2$ were combined with 20 mmol of Cp*MgCl under

(6) Casey, C. P.; Jones, W. D. *J. Am. Chem. Soc.* **1980**, *102*, 6156. Nuttner, G.; Britzinger, H. H.; Bell, L. G.; Friedrich, P.; Bejenke, V.; Neugebauer, D. *J. Organomet. Chem.* **1978**, *145*, 329. Cotton, F. A.; Rusholme, G. A. *J. Am. Chem. Soc.* **1972**, *94*, 402. Calderon, J. L.; Cotton, F. A.; Legzdens, P. *Ibid.* **1969**, *91*, 2528.

(7) Grundke, H.; Paetzold, P. I. *Chem. Ber.* **1971**, *104*, 1136.

(8) Sergeev, N. M. *Prog. Nucl. Magn. Reson. Spectrosc.* **1973**, *9*, 71.

(9) Davison, A.; Rakita, P. E. *Inorg. Chem.* **1970**, *9*, 289.

(10) Benthon, J. E.; Ebsworth, E. A. V.; Moretto, H.; Rankin, D. W. H. *Angew. Chem.* **1972**, *84*, 640.

(11) Paine, R. T.; Light, R. W.; Maier, D. E. *Inorg. Chem.* **1979**, *18*, 368.

(12) Deubzer, B.; Elian, M.; Fischer, E. O.; Fritz, H. P. *Chem. Ber.* **1970**, *103*, 799.

(13) A review of this topic has been presented: Cotton, F. A. "Dynamic Nuclear Magnetic Resonance Spectroscopy"; Jackman, L. M., Cotton, F. A., Eds.; Academic Press: New York, 1975.

(14) Tyler, J. K.; Cox, A. P.; Sheridan, J. *Nature (London)* **1959**, *183*, 1182.

(15) Shibota, S.; Bartell, L. S.; Gavin, R. M. *J. Chem. Phys.* **1964**, *41*, 717.

(16) Almenningen, A.; Haaland, A.; Motzfeldt, T. *J. Organomet. Chem.* **1967**, *7*, 97.

(17) Frasson, E.; Menegus, F.; Panattoni, C. *Nature (London)* **1963**, *199*, 1087. Einstein, F. W. B.; Gilbert, M. M.; Tuck, D. G. *Inorg. Chem.* **1972**, *11*, 2832. Panattoni, C.; Bombieri, G.; Croatto, U. *Acta Crystallogr.* **1966**, *21*, 823.

(18) Bos, K. D.; Bulten, E. J.; Noltes, J. G. *J. Organomet. Chem.* **1975**, *99*, 71.

(19) Jutzi, P.; Kohl, F.; Hofmann, P.; Küger, C.; Tsay, Y. *Chem. Ber.* **1980**, *113*, 757.

(20) Mole, T.; Jeffrey, E. A. "Organoaluminum Compounds"; Elsevier: New York, 1972.

(21) Several references to this topic are found in: Zeigler, K. "Organometallic Chemistry"; Zeiss, H., Ed.; Reinhold: New York, 1960. Eisch, J. J. *Adv. Organomet. Chem.* **1977**, *16*, 67. Oliver, J. P. *Ibid.* **1977**, *16*, 111. Koster, R.; Binger, R. *Adv. Inorg. Chem. Radiochem.* **1965**, *7*, 263. Richards, D. H. *Chem. Soc. Rev.* **1977**, *6*, 235. Egger, K. W.; Cocks, A. T. *J. Am. Chem. Soc.* **1972**, *94*, 1810.

(22) Dolzine, T. W.; Oliver, J. P. *J. Am. Chem. Soc.* **1974**, *96*, 1737. Stucky, G. D.; McPherson, A. M.; Rhine, W. E.; Eisch, J. J.; Considine, J. L. *Ibid.* **1974**, *96*, 1941.

(23) Kasai, P. H.; McLeod, D., Jr.; Watanabe, T. *J. Am. Chem. Soc.* **1977**, *99*, 3521. Kasai, P.; McLeod, D., Jr. *Ibid.* **1975**, *97*, 5609.

(24) Giannini, N.; Cesca, S. *Gazz. Chim. Ital.* **1961**, *91*, 597.

(25) Kroll, W. R.; Naegele, W. *Chem. Commun.* **1969**, 246. Kroll, W. R.; McDivitt, J. R.; Naegele, W. *Inorg. Nucl. Chem. Lett.* **1969**, *5*, 973.

(26) Haaland, A.; Weidlein, J. *J. Organomet. Chem.* **1972**, *40*, 29.

(27) Drew, D. A.; Haaland, A. *Acta. Chem. Scand.* **1973**, *27*, 3735.

(28) Gropen, O.; Haaland, A. *J. Organomet. Chem.* **1975**, *92*, 157. The electron diffraction data do not unambiguously favor the assigned η^2 configuration; however, MO calculations suggested that the η^2 structure is ~ 4 kcal mol⁻¹ more stable than the η^3 structure.

(29) Stadelhofer, J.; Weidlein, J.; Fischer, P.; Haaland, A. *J. Organomet. Chem.* **1976**, *116*, 55.

(30) A preliminary report of this work has appeared: Schonberg, P. R.; Paine, R. T.; Campana, C. F. *J. Am. Chem. Soc.* **1979**, *101*, 7726.

(31) Threlkel, R. S.; Bercaw, J. E. *J. Organomet. Chem.* **1977**, *136*, 1.

Table I. Experimental Data for the X-ray Diffraction Study of $[\text{Cp}^*\text{Al}(\text{Me})\text{Cl}]_2$, 1, and $[\text{Cp}^*\text{Al}(i\text{-Bu})\text{Cl}]_2$, 3

	1	3
(A) Crystal Parameters		
crystal system	monoclinic	monoclinic
space group	$P2_1/c$	$P2_1/n$
a , Å	8.550 (2)	13.040 (6)
b , Å	8.917 (3)	8.928 (2)
c , Å	16.012 (7)	13.083 (3)
β , deg	104.65 (2)	98.06 (3)
V , Å ³	1181.1 (7)	1508.3 (9)
Z	2	2
mol wt	425.4	509.6
$F(000)$	456	552
ρ (calcd), g cm ⁻³	1.20	1.12
(B) Measurement of Intensity Data		
diffractometer	Syntex P3/F	Syntex P3/F
radiation	Mo $K\alpha$ ($\lambda = 0.71069$ Å)	Mo $K\alpha$ ($\lambda = 0.71069$ Å)
monochromator	highly oriented graphite crystal	highly oriented graphite crystal
reflections measd	$^+h, ^+k, \pm l$	$^+h, ^+k, \pm l$
2θ range	3° - 45°	3° - 45°
temp, °C	-65	27
scan type	θ - 2θ	θ - 2θ
scan speed, deg min ⁻¹	8.4-29.3	3.91-29.3
scan range	from $[2\theta(K\alpha_1) - 1.2]^\circ$ to $[2\theta(K\alpha_2) + 1.2]^\circ$	from $[2\theta(K\alpha_1) - 1.0]^\circ$ to $[2\theta(K\alpha_2) + 1.0]^\circ$
bkgd measurement	stationary crystal counter; at beginning and end of 2θ scan—each for half the time taken for the 2θ scan	stationary crystal counter; at beginning and end of 2θ scan—each for half the time taken for the 2θ scan
standard reflections	2 measured every 48 reflections $[2,1,5]$, $[3,1,\bar{1}]$	2 measured every 46 reflections $[3,0,3]$, $[2,\bar{2},2]$
reflections collected	4063 total, yielding 3263, independent reflect	2349 total, yielding 1986, independent reflect
reflections obsd ($I > 3\sigma(I)$)	2255 (65.1%)	1154 (58%)
absorption coeff, cm ⁻¹	3.6	2.9

dry nitrogen in toluene. The reaction mixture was shaken for 5 min and then filtered through a coarse frit Schlenk filter. The collected filtrate was vacuum evaporated, leaving a colorless crystalline solid and a small amount of yellow-orange oil. The mixture was extracted with cold hexane; the majority of the colorless crystalline solid was retained on the frit, and the yellow-orange oil was removed in the filtrate. The recovered yield of 1 is about 50%.³² The solid sublimed with some decomposition at 80 °C.

Alternatively, 1 was prepared from the combination of 10 mmol of $[(\text{CH}_3)_2\text{AlCl}]_2$ and 20 mmol of Cp^*Li in toluene. The mixture was shaken for 10 min, and the yellow-orange slurry was filtered through a coarse frit Schlenk filter. The crude product was recovered by vacuum evaporation of the solvent and purified as described above. The white crystalline solid is extremely air and moisture sensitive, and decomposition is indicated by the formation of a purple oil. The solid is soluble in benzene, toluene, THF, and diethyl ether and slightly soluble in hexane: mass spectrum, m/e (assignment, relative intensity) 232 ($^{36}\text{Cl}_2\text{AlCp}^{*+}$, 4), 212 ($^{36}\text{ClAlCp}^*\text{CH}_3^+$, 80), 197 ($^{36}\text{ClAlCp}^{*+}$, 21), and 177 ($\text{AlCp}^*\text{CH}_3^+$, 100);³³ infrared spectrum (cm⁻¹, KBr pellet) 2940 (s); 2910 (s, br), 2860 (s), 1615 (m), 1560 (w), 1442 (s), 1378 (s), 1265 (w), 1192 (s), 1065 (s), 1030 (m, br), 895 (m), 790 (m), 670 (m, br), 592 (w), 445 (m, br), 334 (m, br); proton NMR (32 °C, benzene) δ 1.87 (relative intensity 5), -0.59 (relative intensity 1); carbon-13 NMR (32 °C, benzene) δ 115.36, 10.74.

Preparation of $[\text{Cp}^*\text{Al}(\text{C}_2\text{H}_5)\text{Cl}]_2$, 2. This compound was prepared in a manner identical with that described for 1 except that $[(\text{C}_2\text{H}_5)_2\text{AlCl}]_2$ was used. The crude product is a yellow solid which can be sublimed at 58 °C providing a colorless crystalline solid. The yellow oil contaminating the crude product also sublimed, and care must be exercised in order to obtain a pure product: mass spectrum, m/e (assignment, relative intensity) 226

$[(\text{C}_2\text{H}_5)\text{AlCp}^*^{36}\text{Cl}^+$, 12), 197 (Cp^*AlCl^+ , 100), 191 ($\text{C}_2\text{H}_5\text{AlCp}^{*+}$, 32);³³ proton NMR (32 °C, benzene) δ 1.87 (relative intensity 5), 1.14 (relative intensity 1, $J_{\text{HH}} = 9$ Hz, t), -0.03 (relative intensity 0.65, $J_{\text{HH}} = 9$ Hz, q); carbon-13 NMR (32 °C, benzene) δ 115.45, 10.88, 10.02.

Preparation of $[\text{Cp}^*\text{Al}(i\text{-C}_4\text{H}_9)\text{Cl}]_2$, 3. This compound could be prepared in a manner identical with that described for 1; however, a simpler, more consistent preparation utilized $[(i\text{-C}_4\text{H}_9)\text{AlCl}]_2$ as the starting material instead of $[(i\text{-C}_4\text{H}_9)_2\text{AlCl}]_2$. Typically, 10 mmol of $[(i\text{-C}_4\text{H}_9)\text{AlCl}]_2$ (25% by weight in hexane) were combined with 20 mmol of Cp^*Li slurried in toluene under dry nitrogen. The mixture was agitated for 5 min and filtered through a coarse frit Schlenk filter. The solvent was removed from the filtrate, leaving a crude yellow-orange semisolid. Purification by extraction with hexane was unsuccessful since the desired product and impurities were soluble in this solvent. Sublimation at 95 °C provided pure, colorless crystals of 3. This material was soluble in benzene, toluene, and hexane, and it is very air and moisture sensitive: mass spectrum m/e (assignment, relative intensity) 254 ($\text{C}_4\text{H}_9\text{AlCp}^*^{36}\text{Cl}^+$, 4), 219 ($\text{C}_4\text{H}_9\text{AlCp}^{*+}$, 15), 197 ($\text{Cp}^*\text{Al}^{36}\text{Cl}^+$, 100);³³ proton NMR (32 °C, benzene) δ 1.87 (relative intensity 5.2), 1.05 (relative intensity 2.0), 0.02 (relative intensity 0.64, $J_{\text{HH}} = 9$ Hz, d); carbon-13 NMR (32 °C, benzene) δ 115.27, 27.84, 25.91, 10.59.

Miscellaneous Reactions. Attempts to prepare RAlCp^*_2 and R_2AlCp^* from $[\text{RAlCl}]_2$ or $[\text{R}_2\text{AlCl}]_2$ and LiCp^* or Cp^*MgCl were unsuccessful. The combination of $[(\text{C}_2\text{H}_5)_2\text{AlCl}]_2$ with LiCp^* in toluene produces a white solid which sublimates at 135 °C; however, it is relatively insoluble in organic solvents. The reaction of Cp^*MgCl with $(\text{C}_2\text{H}_5)_2\text{AlH}$ in toluene was found to produce MgCp^*_2 in good yield. Impurities were removed by extraction with cold hexane, and the remaining colorless solid was sublimed at 60 °C (overall yield 50%). MgCp^*_2 is soluble in toluene and benzene and partially soluble in hexane. Elemental analyses are consistent with the composition $\text{MgC}_{20}\text{H}_{30}$: mass spectrum m/e (assignment, relative intensity) 294 ($^{24}\text{MgCp}^*_2^+$, 0.2), 159 ($^{24}\text{MgCp}^*^+$, 100); proton NMR (32 °C, benzene) δ 1.97; carbon-13 NMR (32 °C, benzene) δ 110.30, 10.07.

Crystal Structure Determinations. A crystal of 1 ($0.25 \times 0.25 \times 0.35$ mm) was obtained by recrystallization from cold hexane; it was lodged in a glass capillary and sealed under argon.

(32) The crude product yield of 1 is much larger (~85%); however, the partial solubility of 1 in hexane is responsible for the reduced yield of the extracted product.

(33) Only the principal ions in the mass spectra are listed here. Ions containing the ^{37}Cl isotope were also observed in the correct intensity ratio, and ions due to the fragmentation of $(\text{CH}_3)_6\text{C}_6$ were easily detected below m/e 137.

Table II. Heavy-Atom Positional Parameters and Their Esd's for $[\text{Cp}^*\text{Al}(\text{CH}_3)\text{Cl}]_2$

atom	x/a	y/b	z/c
Al(1)	1.1707 (1)	0.5084 (1)	0.0899 (1)
Cl(1)	0.8859 (1)	0.4938 (1)	0.0642 (1)
C(1)	1.2207 (4)	0.7377 (4)	0.1122 (2)
C(2)	1.1923 (4)	0.6873 (4)	0.1915 (2)
C(3)	1.3267 (4)	0.5994 (4)	0.2347 (2)
C(4)	1.4378 (4)	0.5963 (4)	0.1834 (2)
C(5)	1.3764 (4)	0.6781 (4)	0.1083 (2)
C(6)	1.1300 (5)	0.8573 (4)	0.0538 (2)
C(7)	1.0536 (5)	0.7348 (5)	0.2268 (3)
C(8)	1.3461 (6)	0.5193 (5)	0.3184 (3)
C(9)	1.5920 (4)	0.5079 (4)	0.2053 (3)
C(10)	1.4596 (5)	0.7106 (5)	0.0376 (3)
C(11)	1.2345 (4)	0.3027 (4)	0.1167 (2)

The data were collected at -65°C . A crystal of **3** ($0.40 \times 0.15 \times 0.40$ mm) was obtained by sublimation; it was mounted in a glass capillary and sealed under argon. The data were collected at 25°C . Each crystal was centered on a Syntex P3/F automated diffractometer, and the determinations of the crystal class, orientation matrix, and accurate unit cell parameters were performed in a standard manner.³⁴ The data for both crystals were obtained by the θ - 2θ technique using Mo $K\alpha$ radiation, a scintillation counter, and a pulse height analyzer. Details of the data collections are summarized in Table I. Inspection of the collected data for **1** revealed systematic absences $l = 2n + 1$ for $h0l$ and $k = 2n + 1$ for $0k0$, and the monoclinic space group $P2_1/c$ was indicated. For **3**, the systematic absences $h + l = 2n + 1$ for $h0l$ and $k = 2n + 1$ for $0k0$ indicated the monoclinic space group $P2_1/n$. The maximum and minimum transmission factors for **1** and **3** are 0.915 and 0.882 and 0.957 and 0.890, respectively, and corrections for absorption were found to unnecessary. Redundant and equivalent reflection data were averaged and converted to unscaled $|F_o|$ values following corrections for Lorentz and polarization effects.

Solution and Refinement of the Structures. The calculations were performed on a Syntex R3/XTL structure determination system.³⁴ Scattering factors for Al, Cl, and C atoms were taken from the compilation of Cromer and Waber,³⁵ while those for hydrogen were taken from Stewart and co-workers.³⁶ Both real ($\Delta f'$) and imaginary ($\Delta f''$) components of the anomalous dispersion were included for the Al and Cl atoms by using the values listed by Cromer and Liberman.³⁷ The function minimized during the least-squares refinement was $\sum w(|F_o| - |F_c|)^2$.

Both structures were solved by direct methods using the program MULTAN.³⁸ Normalized structure factor amplitudes were generated in a standard manner from $|F_o(hkl)|$ values. For both **1** and **3** the statistical distributions of $|E|$ values were consistent with those expected for centrosymmetric crystals. In each case the E map generated from the phase set with the best combined figure of merit yielded a chemically reasonable solution from which the coordinates of the aluminum and chlorine atoms were ascertained. Subsequent Fourier syntheses revealed the locations of all remaining nonhydrogen atoms in the structure. The positional and individual isotropic thermal parameters of the nonhydrogen atoms were refined by using a block-diagonal least-squares procedure.

At this point, in both structure solutions, the coordinates of the hydrogen atoms were calculated in idealized positions. In-

Table III. Heavy-Atom Positional Parameters and Their Esd's for $[\text{Cp}^*\text{Al}(i\text{-C}_4\text{H}_9)\text{Cl}]_2$

atom	x/a	y/b	z/c
Al(1)	0.6250 (2)	0.5396 (3)	0.4664 (2)
Cl(1)	0.4682 (2)	0.3999 (3)	0.3990 (2)
C(1)	0.6058 (7)	0.7132 (10)	0.3575 (6)
C(2)	0.6671 (7)	0.6175 (9)	0.3051 (6)
C(3)	0.7674 (7)	0.6205 (9)	0.3551 (6)
C(4)	0.7717 (7)	0.7197 (9)	0.4388 (6)
C(5)	0.6721 (7)	0.7770 (9)	0.4412 (6)
C(6)	0.4972 (8)	0.7678 (12)	0.3166 (8)
C(7)	0.6241 (10)	0.5301 (13)	0.2067 (7)
C(8)	0.8564 (9)	0.5309 (13)	0.3244 (8)
C(9)	0.8691 (8)	0.7586 (12)	0.5142 (9)
C(10)	0.6424 (8)	0.9057 (11)	0.5057 (8)
C(11)	0.7080 (7)	0.3633 (9)	0.5104 (6)
C(12)	0.8086 (7)	0.3711 (10)	0.5857 (7)
C(13)	0.8594 (9)	0.2201 (4)	0.6058 (9)
C(14)	0.7947 (9)	0.4422 (3)	0.6887 (8)

dividual anisotropic thermal parameters were then assumed for all nonhydrogen atoms. Several cycles of full-matrix least-squares refinement were then carried out in which the positions of all hydrogen atoms were fixed and the thermal parameters of the nonhydrogen atoms were allowed to vary anisotropically. Final values of R_F , R_{wF} , and GOF were 0.061, 0.092, and 1.241 for **1** and 0.075, 0.095, and 1.1783 for **3**.³⁹ Final difference Fourier syntheses revealed no unusual features. Tables of observed and calculated structure factor amplitudes are available (Tables S-1 and S-2).⁴⁰ The atomic positional parameters for **1** and **3** are collected in Tables II and III, respectively. The hydrogen atom positions (Tables S-3 and S-4) and all thermal parameters (Tables S-5 and S-6) are available.⁴⁰

MO Calculations. The computational method employed is an approximate Hartree-Fock-Roothaan SCF-LCAO molecular orbital calculation developed by Fenske and Hall⁴¹ and locally modified to run on the University IBM-360 computer system. The method is parameter free and self-consistent and depends only on the atomic coordinates and choice of wave functions as input data. For computational expediency the calculation was performed on the model compound $[\text{CpAl}(\text{CH}_3)\text{Cl}]_2$. The substitution of the Cp ring for the Cp* ring in **1** may be expected to alter slightly the starting Cp ligand orbital energies.⁴² However, the orbital energy shifts do not appear to significantly alter the qualitative results of the calculations. The calculations were iterated until the absolute value of the difference in the Mulliken population in each valence orbital was less than 0.001. The basis functions were the double- ζ functions of Clementi.⁴³ The 2s functions were curve fit to single- ζ form while being held orthogonal to a similarly constructed 1s function. The 2p and 3s functions for Cl and Al atoms were constructed in the same fashion while the carbon 2p orbitals were held in their original form. The interatomic distances and angles used were obtained from the structure determination of **1**. The bond lengths and angles were idealized to conform to C_{2v} symmetry. A description of the master and local coordinate systems is given in Table S-9.⁴⁰

Results and Discussion

In the current study, the reactions of $(\text{CH}_3)_5\text{C}_5\text{Li}$ and $(\text{CH}_3)_5\text{C}_5\text{MgCl}$ with $[(\text{CH}_3)_2\text{AlCl}]_2$, $[(\text{C}_2\text{H}_5)_2\text{AlCl}]_2$, $[(\text{C}_2\text{-H}_5)\text{AlCl}_2]_2$, $[(i\text{-C}_4\text{H}_9)_2\text{AlCl}]_2$, $[(i\text{-C}_4\text{H}_9)\text{AlCl}]_2$, and $[(\text{C}_2\text{-H}_5)_2\text{AlH}]_2$ were investigated, and the results of these re-

(34) Hardware configuration for the P3/F diffractometer and the R3/XTL system has been described: Campana, C. F.; Shepard, D. F.; Litchman, W. M. *Inorg. Chem.* 1981, 20, 4039. Programs used for centering of reflections, autoindexing, refinement of cell parameters, axial photographs, data collection, data reduction, Fourier synthesis, block-diagonal and full-matrix least-squares refinement, bond length and bond angle calculations, error analysis, least-squares planes calculations, direct-methods structure solution, and calculation of hydrogen atom positions are those described in: "Syntex R3 Operations Manual"; Sparks, R. A. Ed.; Syntex Analytical Instruments: Cupertino, CA 1978.

(35) Cromer, D. T.; Waber, J. T. *Acta Crystallogr., Sect. B* 1965, B18, 104.

(36) Stewart, R. F.; Davidson, R. F.; Simpson, W. T. *J. Chem. Phys.* 1965, 42, 3175.

(37) Cromer, D. T.; Liberman, D. J. *J. Chem. Phys.* 1970, 53, 1891.

(38) Germain, G.; Main, P.; Woolfson, M. M. *Acta Crystallogr., Sect. A* 1971, A27, 368.

(39) Discrepancy indices used in the text are defined as follows: $R_F(\%) = [\sum ||F_o| - |F_c||] / \sum |F_o| \times 100$; $R_{wF}(\%) = [\sum w(|F_o| - |F_c|)^2] / \sum w|F_o|^2]^{1/2} \times 100$. The "goodness of fit" (GOF) is defined as $\text{GOF} = [\sum w(|F_o| - |F_c|)^2 / (\text{NO} - \text{NV})]^{1/2}$, where NO is the number of observations and NV is the number of variables.

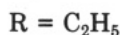
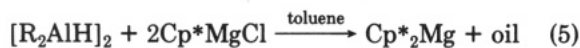
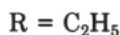
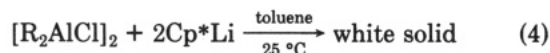
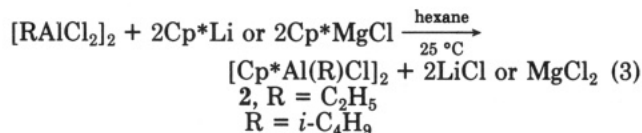
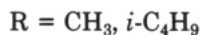
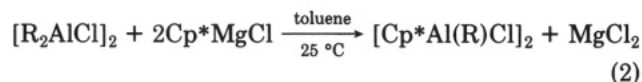
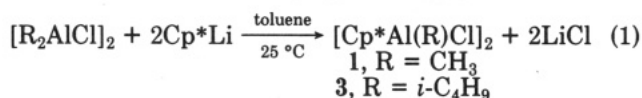
(40) Supplementary material.

(41) Hall, M. B.; Fenske, R. F. *Inorg. Chem.* 1972, 11, 768. Fenske, R. F. *Prog. Inorg. Chem.* 1976, 21, 179.

(42) Lichtenberger, D. L., private communication. Calabro, D. C.; Hubbard, J. L.; Blevins, C. H.; Campbell, A. C.; Lichtenberger, D. L. *J. Am. Chem. Soc.* 1981, 103, 6839.

(43) Clementi, E. *J. Chem. Phys.* 1964, 40, 1944.

actions are summarized by eq 1–5. In contrast to earlier



reports on reaction systems combining NaCp and alkyl-aluminum halides,^{24–26} the pentamethylcyclopentadienide reagents did not appear to produce detectable amounts of trialkylaluminum derivatives, Cp*AlR₂. The new crystalline products [Cp*Al(R)Cl]₂ were obtained in good yields from the oily reaction mixtures by extraction or sublimation procedures, and they were found to be soluble in benzene, toluene, and THF and slightly soluble in cold hexane. The purified products were extremely air and moisture sensitive. The combination of LiCp* and [(C₂H₅)₂AlCl]₂ unexpectedly produced a relatively insoluble white solid. The reactivity and insolubility of the compound so far have prohibited complete characterization. The combination of [(C₂H₅)₂AlH]₂ with Cp*MgCl led to the formation of MgCp*₂ in high yields by a complex reaction process which has not been fully elucidated.

Spectroscopic Characterization. The mass spectra of [Cp*Al(CH₃)Cl]₂ (1), [Cp*Al(C₂H₅)Cl]₂ (2), and [Cp*Al(*i*-C₄H₉)Cl]₂ (3) are similar. The most intense ions were Cp*Al(R)Cl⁺, Cp*AlCl⁺, Cp*AlR⁺, and Cp*⁺ and its fragments. The relative intensities of these ions varied for the three compounds, and in no case was a parent ion detected with 70-eV ionizing energy. Only in 1 was an ion, Cp*AlCl₂⁺, detected which suggested that the gas-phase species might be dimeric. Consequently, the mass spectra, under the strenuous ionizing conditions available, did not provide an unambiguous assignment of the molecular weight of the gaseous neutral molecules. For MgCp*₂, on the other hand, a weak parent ion was observed.

The ¹H and ¹³C{¹H} NMR data for 1–3 are related. Carbon-13 resonances at 115.36 (1), 115.45 (2), 115.27 (3) and 10.74 (1), 10.88 (2), 10.59 (3) ppm were assigned to the Cp* ring carbon atoms and Cp* terminal methyl groups. A ¹³C resonance for the methyl group attached directly to the aluminum atom in 1 was not detected. A similar absence was found earlier for the methyl groups on CpAl(CH₃)₂.⁴⁴ For 2 a ¹³C resonance was detected at 10.02 ppm, and it was assigned to the methyl carbon atom of the terminal ethyl group. A resonance for the α-carbon atom of the ethyl group was not observed. Similarly for 3, the resonance for the α-carbon atom of the isobutyl group was not observed; however, resonances at 27.84 and 25.91 ppm

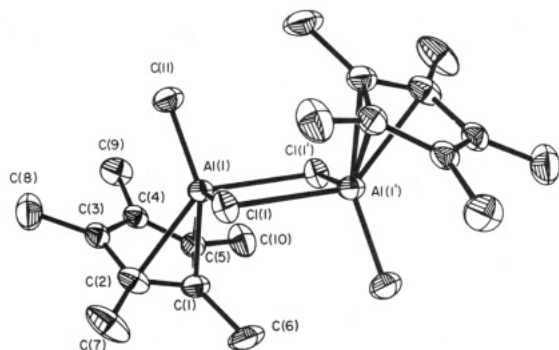


Figure 1. Molecular structure and labeling scheme of the atoms in [Cp*Al(CH₃)Cl]₂ (50% probability ellipsoids).

were observed and assigned to the methyl carbon and β-carbon atoms, respectively. Similar alkyl group resonances were found in [(*i*-C₄H₉)₂AlCl]₂. The ¹³C resonances for 4 appear at 110.30 ppm (ring carbon atoms) and 10.07 ppm (ring methyl groups).

In 1–3, the ¹H spectra showed a singlet at 1.87 ppm (relative intensity 5) which was assigned to equivalent methyl groups on the Cp* rings in each compound. In addition, 1 showed a singlet at –0.59 ppm (relative intensity 1) which was assigned to the protons of the methyl group bonded directly to the Al atom, 2 displayed a triplet at 1.14 ppm (*J*_{HH} = 9 Hz, relative intensity 1.0) and a quartet at –0.03 ppm (*J*_{HH} = 9 Hz, relative intensity 0.7) which were assigned to the ethyl group methyl and methylene carbon atoms, and 3 showed a doublet at 1.05 ppm (*J*_{HH} = 9 Hz, relative intensity 2.0) and a doublet at 0.02 ppm (*J*_{HH} = 8 Hz, relative intensity 0.6) which were assigned to the six equivalent isobutyl group methyl hydrogen atoms and the α-methylene hydrogen atoms, respectively. The multiplet expected for the proton resonance of the tertiary CH group was not detected. The ¹H spectrum for 4 showed a single resonance at 1.97 ppm.

Although the available spectroscopic data are consistent with the proposed chemical formulations of 1–3 as [Cp*Al(R)Cl]_x, they did not permit us to distinguish between monomeric, dimeric, or oligomeric structures. In addition, the hapticity of the Cp* ring could not be determined from the chemical shifts⁴⁵ and splitting patterns. The apparent equivalence of the Cp* ring carbon atoms and the Cp* methyl carbon and hydrogen atoms at 32 °C may result from rapid 1,2 or 1,3 sigmatropic shifts between η¹, η², or η³ structures or from rapid ring whizzing.¹³ Attempts to detect a static structure in 1 at –80 °C by ¹H NMR spectroscopy revealed no appreciable alteration in the ring methyl ¹H line shape when compared to the resonance line width measured at 32 °C. Similar dynamic behavior has been demonstrated for several pentamethylcyclopentadienyl compounds including η¹-Cp*Ge(CH₃)₃ and η¹-Cp*Sn(CH₃)₃.⁹

The detailed character of the structure of 4 also is uncertain. Elemental analysis and the mass spectrum are consistent with a monomeric Cp*₂Mg formulation similar to the known Cp₂Mg compound. The NMR spectra show that the ring carbon and proton atoms are equivalent on the NMR time scale at 32 °C and ¹H NMR spectra recorded at –80 °C showed no appreciable line broadening in toluene solution.

(45) Attempts to correlate Cp ring chemical shifts with ring hapticity by Sergeyev and co-workers^{8,46} are not reliable in all cases.⁴⁴ The crystal structures of 1 and 3 provide further examples of the care with which chemical shift–hapticity correlations should be treated.

(46) Grishin, Y. K.; Sergeyev, N. M.; Ustynuk, Y. A. *Org. Magn. Reson.* 1972, 4, 377.

(44) Fisher, P.; Stadelhofer, J.; Weidlein, J. *J. Organomet. Chem.* 1976, 116, 65.

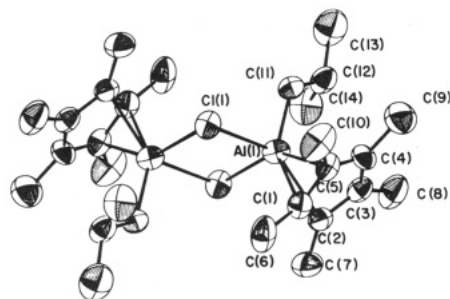


Figure 2. Molecular structure and labeling scheme of the atoms in $[\text{Cp}^*\text{Al}(i\text{-C}_4\text{H}_9)\text{Cl}]_2$ (50% probability ellipsoids).

Table IV. Selected Interatomic Distances (Å) and Their Esd's for $[\text{Cp}^*\text{Al}(\text{CH}_3)\text{Cl}]_2^a$

A. Bonded Distances			
Al(1)–Cl(1)	2.369 (1)	C(4)–C(5)	1.390 (4)
Al(1)–Cl(1')	2.392 (1)	C(5)–C(1)	1.449 (5)
Al(1)–C(1)	2.100 (3)	C(1)–C(6)	1.499 (5)
Al(1)–C(2)	2.252 (3)	C(2)–C(7)	1.499 (5)
Al(1)–C(5)	2.282 (3)	C(3)–C(8)	1.490 (5)
C(1)–C(2)	1.424 (5)	C(4)–C(9)	1.499 (5)
C(2)–C(3)	1.418 (5)	C(5)–C(10)	1.510 (5)
C(3)–C(4)	1.405 (5)	Al(1)–C(11)	1.931 (3)
B. Nonbonded Distances			
Al(1)–Al(1')	3.548 (1)	Al(1)–C(6)	3.168 (4)
Cl(1)–Cl(1')	3.175 (1)	Al(1)–C(7)	3.315 (5)
Al(1)–C(3)	2.499 (3)	Al(1)–C(10)	3.332 (4)
Al(1)–C(4)	2.518 (3)		

^a Primes indicate the symmetry operation $2 - x, 1 - y, -z$.

Crystal Structures. The X-ray diffraction analyses for **1** and **3** indicate that the molecules are dimeric in the solid state with formulations $[\text{Cp}^*\text{Al}(\text{R})\text{Cl}]_2$. Views of the dimeric units are shown in Figures 1 and 2. Selected interatomic bond distances and angles are presented in Tables IV and VI and V and VII, respectively. Least-squares planes and atomic deviations from the planes are presented in the supplementary material (Tables S-7 and S-8).

The molecular structures of **1** and **3** contain a four-membered Al_2Cl_2 ring with planar trans Cp^* rings and trans alkyl groups (CH_3 or $i\text{-C}_4\text{H}_9$). Each dimeric unit possesses crystallographic C_i site symmetry, and the molecules nearly conform to an idealized $C_{2h}-2/m$ geometry. The Al_2Cl_2 rings are slightly asymmetric with the greater asymmetry occurring in **3**. The Al–Cl bridge bond distances in **1**, Al(1)–Cl(1) = 2.369 (1) Å and Al(1)–Cl(1') = 2.392 (1) Å, and in **3**, Al(1)–Cl(1) = 2.451 (4) Å and Al(1)–Cl(1') = 2.340 (3) Å, are long compared with the less accurately known Al–Cl bridge bond distances in $[\text{CH}_3\text{-AlCl}_2]_2$, 2.25 (1) Å and 2.26 (1) Å,⁴⁷ and in $[(\text{CH}_3)_2\text{AlCl}]_2$, 2.31 (3) Å.⁴⁸ The ring angles Al(1)–Cl–Al(1'), **1**, 96.34 (4)° and **3**, 96.1 (1)°, are enlarged over the related angle in $[\text{CH}_3\text{AlCl}_2]_2$, 91.1°.⁴⁷ The nonbonding distances Cl(1)–Cl(1') in **1**, 3.175 (1) Å, and **3**, 3.203 (3) Å, are comparable to the related distances in $[\text{CH}_3\text{AlCl}_2]_2$, 3.16 Å⁴⁷ and $[(\text{C}-\text{H}_3)_2\text{AlCl}]_2$, ~ 3.2 Å,⁴⁸ while the Al(1)–Al(1') distances in **1**, 3.548 (1) Å, and **3**, 3.565 (4) Å, are longer than this distance in $[\text{CH}_3\text{AlCl}_2]_2$, 3.22 Å.⁴⁷ Stuckey and Ross⁴⁹ have compared bond lengths and angles for 17 compounds

containing M_2Cl_2 rings. A linear relationship between the average M–Cl bond distance and the secant of half the M–Cl–M angles was derived, and it was proposed that the ring geometries are dominated by Cl–Cl and M–M repulsions. **1** and **3** are found to fit this correlation which suggests that the central Al_2Cl_2 geometries are probably determined by Al...Al and Cl...Cl nonbonded interactions. The Al– CH_3 and Al– $\text{CH}_2\text{R}'$ bond distances, 1.931 (3) Å and 1.951 (8) Å, fall within the expected range for Al–C (terminal) bond distances.⁵⁰

The Cp^* ring carbon atoms in **1** and **3** are coplanar with maximum deviations of 0.004 and 0.005 Å, respectively. The Cp^* ring methyl groups deviate slightly from the ring planes in probable response to small nonbonded interactions and electronic (orbital overlap) effects. In **1**, C(6), C(7), and C(10) are bent out of the C_5 plane and away from Al(1) by 0.280 (4), 0.146 (5), and 0.074 (4) Å, and C(8) and C(9) are bent out of the C_5 plane and toward Al(1) by 0.058 (5) and 0.069 (4) Å. In **3**, the deviations appear to be less regular; C(6), C(7), C(9), and C(10) are bent out of the C_5 plane and away from Al(1) by 0.299 (11), 0.049 (11), 0.021 (11), and 0.237 (10) Å while C(8) is bent out of the C_5 plane and slightly toward Al(1) by 0.029 (11) Å. Analysis of the angles between the various atomic planes shows that there are more pronounced deviations from ideal $C_{2h}-2/m$ symmetry in **3** than in **1**. In **1**, the planes containing Al(1), Al(1'), and C(1) and Al(1), Al(1'), and C(11) are nearly perpendicular (93.5° and 89.3°) to the Al_2Cl_2 plane, and the angle between the first two planes is 4.2°. In **3**, the angles between the same sets of planes are 99.3°, 81.1°, and 18.2°. In **1**, the angle between the normals to the Al_2Cl_2 plane and the Cp^* ring plane is 142.8° while in **3** this angle is 145.4°.

The stereochemistry involving the aluminum atom and the Cp^* ring is unexpected and unusual. In both **1** and **3**, there are three short aluminum atom–ring carbon atom distances: **1**, Al–C(1) = 2.100 (3) Å, Al–C(2) = 2.252 (3) Å, Al–C(5) = 2.282 (3) Å; **3**, Al–C(1) = 2.096 (9) Å, Al(1)–C(2) = 2.359 (8) Å, Al(1)–C(5) = 2.243 (8) Å. These distances fall within a range expected for Al–C (terminal) and Al–C (electron-deficient bridge) bonding interactions in alkylaluminum compounds.^{47,48,50} The Al–ring plane distances are 1.951 Å (**1**) and 1.988 Å (**3**). The distances Al–C(3) = 2.499 (3) Å and Al–C(4) = 2.518 (3) Å in **1** and Al–C(3) = 2.616 (9) Å and Al–C(4) = 2.563 (9) Å in **3**, on the other hand, are long compared with the accepted range of Al–C bonds, and they are considered to be nonbonding distances. Consequently, the bonding and nonbonding distances in **1** indicate that the Cp^* ring coordination with the aluminum atoms can be considered to be η^3 . In **3**, the Al–C(1) and Al–C(5) distances are essentially the same as the corresponding distances in **1**; however, Al–C(2) is about 0.1 Å longer in **3** than in **1**. It appears that the "slippage" of the aluminum atom and the rotation of the Cp^* in **3** bring that molecule to an intermediate $\eta^2-\eta^3$ configuration. Nonbonded interactions resulting from this placement of the RAlCl_2 group may be responsible for the already noted displacement of C(6), C(7), C(9), and C(10) out of the Cp^* plane away from the Al atom. Nonbonded distances listed in Tables IV and VI for the Al... CH_3 (ring) separations show that Al...C(6) distances are less than the sum of the van der Waal radii for an Al atom and a CH_3 group,⁵¹ 3.25 Å, and the Al...C(7) and Al...C(10) separations are only slightly longer than 3.25 Å. In addition, it is curious that the Al...C(12) distance is short 3.064 (9) Å.

(47) Allegra, G.; Perego, G.; Immirzì, A. *Makromol. Chem.* **1973**, *61*, 69.

(48) Brockway, L. O.; Davidson, N. R. *J. Am. Chem. Soc.* **1941**, *63*, 3287.

(49) Ross, F. K.; Stucky, G. D. *J. Am. Chem. Soc.* **1970**, *92*, 4538.

(50) Oliver, J. P. *Adv. Organomet. Chem.* **1977**, *15*, 235.

(51) Pauling, L. "The Nature of the Chemical Bond"; Cornell University Press: Ithaca, N.Y., 1960; p 261.

Table V. Selected Interatomic Angles (Deg) and Their Esd's for $[\text{Cp}^*\text{Al}(\text{CH}_3)\text{Cl}]_2$

$\text{Cl}(1)-\text{Al}(1)-\text{Cl}(1')$	83.66 (4)	$\text{C}(5)-\text{C}(1)-\text{C}(2)$	106.7 (3)	$\text{C}(5)-\text{C}(1)-\text{C}(6)$	124.7 (3)	$\text{C}(2)-\text{C}(1)-\text{C}(6)$	127.1 (3)
$\text{Al}(1)-\text{Cl}(1)-\text{Al}(1')$	96.34 (4)	$\text{C}(1)-\text{C}(2)-\text{C}(3)$	108.0 (3)	$\text{C}(1)-\text{C}(2)-\text{C}(7)$	125.2 (3)	$\text{C}(3)-\text{C}(2)-\text{C}(7)$	126.4 (3)
$\text{Cl}(1)-\text{Al}(1)-\text{C}(11)$	101.9 (1)	$\text{C}(2)-\text{C}(3)-\text{C}(4)$	108.0 (3)	$\text{C}(2)-\text{C}(3)-\text{C}(8)$	126.6 (3)	$\text{C}(4)-\text{C}(3)-\text{C}(8)$	125.4 (3)
$\text{Al}(1)-\text{Al}(1)-\text{C}(11)$	105.6 (1)	$\text{C}(3)-\text{C}(4)-\text{C}(5)$	109.4 (3)	$\text{C}(3)-\text{C}(4)-\text{C}(9)$	123.9 (3)	$\text{C}(5)-\text{C}(4)-\text{C}(9)$	126.6 (3)
$\text{C}(11)-\text{Al}(1)-\text{C}(1)$	148.6 (1)	$\text{C}(4)-\text{C}(5)-\text{C}(1)$	107.8 (3)	$\text{C}(4)-\text{C}(5)-\text{C}(10)$	127.0 (3)	$\text{C}(1)-\text{C}(5)-\text{C}(10)$	125.0 (3)

Table VI. Selected Interatomic Distances (Å) and Their Esd's for $[\text{Cp}^*\text{Al}(i\text{-C}_4\text{H}_9)\text{Cl}]_2$

A. Bonded Distances			
$\text{Al}(1)-\text{Cl}(1)$	2.451 (4)	$\text{C}(6)-\text{C}(1)$	1.525 (13)
$\text{Al}(1)-\text{Cl}(1')$	2.340 (3)	$\text{C}(7)-\text{C}(2)$	1.542 (12)
$\text{Al}(1)-\text{C}(1)$	2.096 (9)	$\text{C}(8)-\text{C}(3)$	1.509 (14)
$\text{Al}(1)-\text{C}(2)$	2.359 (8)	$\text{C}(9)-\text{C}(4)$	1.534 (14)
$\text{Al}(1)-\text{C}(5)$	2.243 (8)	$\text{C}(10)-\text{C}(5)$	1.507 (13)
$\text{Al}(1)-\text{C}(11)$	1.951 (8)		
$\text{C}(1)-\text{C}(2)$	1.412 (12)	$\text{C}(11)-\text{C}(12)$	1.528 (12)
$\text{C}(2)-\text{C}(3)$	1.379 (13)	$\text{C}(12)-\text{C}(13)$	1.509 (15)
$\text{C}(3)-\text{C}(4)$	1.403 (12)	$\text{C}(12)-\text{C}(14)$	1.523 (14)
$\text{C}(4)-\text{C}(5)$	1.401 (12)		
$\text{C}(5)-\text{C}(1)$	1.416 (12)		
B. Nonbonded Distances			
$\text{Al}(1)-\text{Al}(1')$	3.565 (4)	$\text{Al}(1)-\text{C}(12)$	3.064 (9)
$\text{Cl}(1)-\text{Cl}(1')$	3.203 (3)	$\text{Al}(1)-\text{C}(6)$	3.144 (11)
$\text{Al}(1)-\text{C}(3)$	2.616 (9)	$\text{Al}(1)-\text{C}(7)$	3.397 (9)
$\text{Al}(1)-\text{C}(4)$	2.563 (9)	$\text{Al}(1)-\text{C}(10)$	3.311 (10)

The average C-C bond distances for the Cp^* rings in **1**, 1.417 and **3** 1.40 Å, are comparable to the average C-C bond distances in Cp^*_2Fe , 1.419 Å.⁵² The bond length variations in the Cp^* rings of **1** and **3** also are of interest. With respect to the mean C-C bond distance in a η^5 structure, η^3 coordination of a metal atom with Cp^* might be expected to produce lengthening of two C-C ring distances ($\text{C}(1)-\text{C}(2)$ and $\text{C}(1)-\text{C}(5)$) and shortening of the remaining three C-C ring distances. An analysis of the variance on all Cp^* C-C bond lengths in **1** indicates that the C-C distances are not equal at the 95% confidence level, while in **3** the distances are not equal at the 75% confidence level.⁵³ In each case, the C-C distances fall into two groups: long $\text{C}(1)-\text{C}(2)$ and $\text{C}(1)-\text{C}(5)$ distances and short $\text{C}(2)-\text{C}(3)$, $\text{C}(3)-\text{C}(4)$, and $\text{C}(4)-\text{C}(5)$ distances. Lastly, the internal C-C-C ring angles range in **1** from 106.7 (3)° to 109.4 (3)° and in **3** from 107.1 (7)° to 108.8 (7)°. These angles compare favorably with the expected internal angle, 108°, for a planar pentagon.

Several similarities and differences in the structures of **1** and **3** compared to structures of other metalloids and metal Cp compounds are of interest. As mentioned earlier, Haaland and co-workers^{27,28} assigned an η^2 structure for monomeric, gaseous $\text{CpAl}(\text{CH}_3)_2$ (**5**) based upon electron diffraction analysis. The average Al-C(1) and Al-C(2) distance in **5**, 2.21 (2) Å, is intermediate in comparison to the Al-C(1), Al-C(2), and Al-C(5) distances in **1** and **3**. The average ring C-C bond distance in **5**, 1.422 (2) Å, is similar to the average ring C-C bond distances in **1** and **3**. Oliver and co-workers⁵⁴ have recently determined the solid-state structure of **5**, and an infinite chain of $\text{Al}(\text{CH}_3)_2$ units bonded to bridging Cp ligands was found. Unlike Cp_2Pb , which contains an infinite chain of Pb atoms each bonded in a η^5 fashion to two bridging Cp rings, each aluminum atom in **5** appears to bond in a η^1 fashion to two Cp rings. The Al atom lies directly above one carbon atom of each planar Cp ring with Al-C(1)-H, 92°. The solid-

state structure of **5** also resembles the structure of $\text{CpGa}(\text{CH}_3)_2$.⁵⁵ For comparison, the Al-C(1)-C(6) angle is 122.4 (2)° in **1** and 119.76 (6)° in **3**.

It is also interesting to consider the structures of these molecules in a context presented by Hoffman and co-workers⁴ for describing haptotropic shifts of groups $\text{X} = \text{H}^+$, CH_3^+ , CH_2^{2+} , and $\text{Mn}(\text{CO})_3^+$ across a Cp ring. In that study, the relative energies of η^1 , η^3 , η^5 , and η^2 configurations and the energetics of the transit from one configuration to the next were considered. Although an X group of the form AlR_2 or AlClR was not examined in detail, CpBH_2 was noted to be isoelectronic and presumably related to CpCH_2^+ . In the case of CpCH_2^+ , the calculated lowest energy structure was η^2 , and an η^5 structure was the most unstable. Apparently **5** adopts the η^2 structure in the gas phase but not in the solid state. The η^3 configuration in **1** and the slipped η^3 configuration in **3** represent unexpected structures which may derive some of their stability from the Al_2Cl_2 structural unit not present in the other molecules. We have also noted earlier³⁰ that the structure of **1** closely resembles the structure of benzvalene, bicyclo[3.1.0]hex-3-en-2-yl cation, and its rearrangement transients. It appears that the alkylaluminum fragment is capable of stabilizing a η^3 configuration which must have only a brief lifetime in the organic carbocation system.

MO Calculations. In order to better understand the electronic structure and bonding in **1** and **3**, we performed nonparametrized MO calculations⁴¹ on a model compound, $[\text{CpAl}(\text{CH}_3)\text{Cl}]_2$.⁵⁶ The molecule was assigned an idealized C_{2h} structure, and atomic coordinates and bond distances and angles were derived from the structure of **1**. A free Cp^- ligand calculation was performed first in order to determine the eigenvectors required to transform the final canonical molecular orbitals to a basis set of free ligand orbitals.⁵⁷ A calculation for the free Cp^- fragment in D_{5h} symmetry has been reported,^{58,59} however, the structures for **1** and **3** required that the Cp fragment conform to C_{2v} symmetry. The results of the calculation for the three highest filled and two lowest unoccupied MOs are available (Table S-10).^{40,60}

In $[\text{CpAl}(\text{CH}_3)\text{Cl}]_2$ the fragments Al^{3+} , Cl^- , CH_3^- , and C_5H_5^- were combined, and the low site symmetry at the aluminum atom gave rise to significant orbital mixing.⁶¹

(55) Mertz, K.; Zettler, F.; Hausen, F. D.; Weidlein, J. *J. Organomet. Chem.* 1976, 122, 159.

(56) It has been recently shown that substitution of hydrogen atoms by methyl groups on a Cp ring can alter the observed ionization energies in $\text{CpMn}(\text{CO})_3$.⁴² Therefore, it was anticipated that the use of C_5H_5^- in the present calculation for computational expediency would slightly alter the starting orbital energies for the ring. However, it is observed that the Cp orbital energy shifts do not significantly alter the qualitative results of the calculation.

(57) This transformation process has been shown to aid the interpretation of the frontier orbital interactions, as well as assist in the comparison of results for related molecules.⁵⁸

(58) Lichtenberger, D. L.; Fenske, R. F. *J. Am. Chem. Soc.* 1976, 98, 50.

(59) Peterson, J. L.; Lichtenberger, D. L.; Fenske, R. F.; Dahl, L. F. *J. Am. Chem. Soc.* 1975, 97, 6433.

(60) The a''_2 Cp⁻ MO in D_{5h} symmetry becomes the $1b_1$ MO in C_{2v} symmetry. The e''_1 orbital is split into the $2b_1$ and $1a_2$ orbitals, and the e''_2 is split into the $3b_1$ and $2a_2$ orbitals. The results of the calculation in C_{2v} symmetry compare favorably with those reported in D_{5h} .⁵⁸

(52) Freyberg, D. D.; Robbins, J. L.; Raymond, K. N.; Smart, J. C. *J. Am. Chem. Soc.* 1979, 101, 892.

(53) Hamilton, W. C. "Statistics in Physical Science"; Ronald Press: New York, 1964; Chapter 3.

(54) Teclé, B.; Corfield, P. W. R.; Oliver, J. P. *Inorg. Chem.* 1982, 21, 458.

Table VII. Selected Interatomic Angles (Deg) and Their Esd's for $[\text{Cp}^*\text{Al}(i\text{-C}_4\text{H}_9)\text{Cl}]_2$

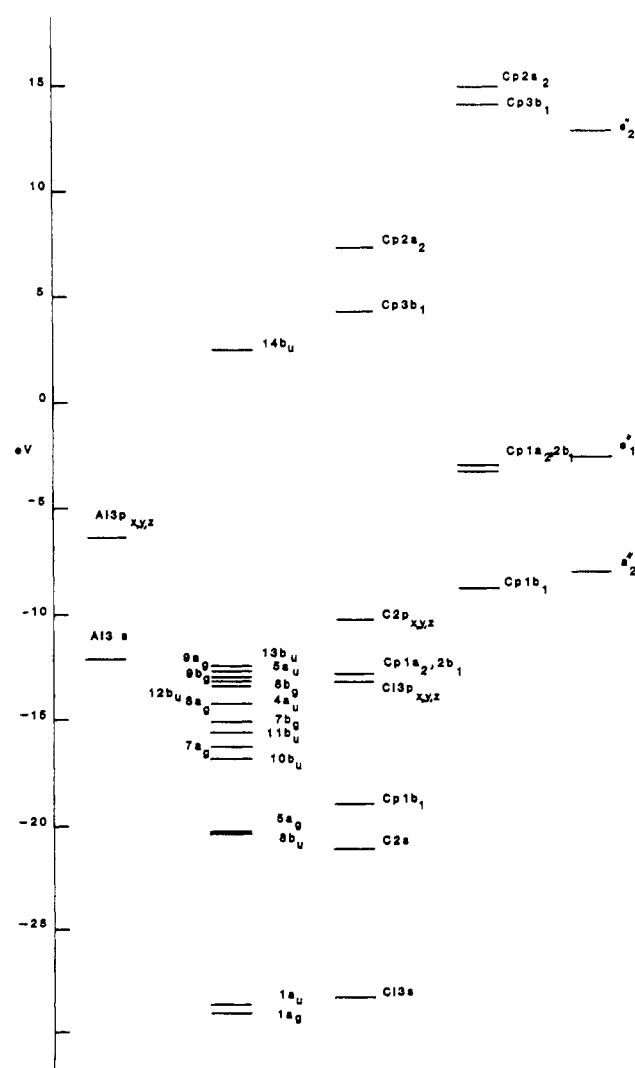
Cl(1)-Al(1)-Cl(1')	83.9 (1)	Al(1)-C(11)-C(12)	123.0 (6)	C(5)-C(1)-C(2)	107.1 (7)	C(5)-C(1)-C(6)	125.2 (8)
Al(1)-Cl(1)-Al(1')	96.1 (1)	C(11)-C(12)-C(13)	112.9 (8)	C(1)-C(2)-C(3)	108.8 (8)	C(1)-C(2)-C(7)	123.2 (8)
Cl(1)-Al(1)-C(11)	95.5 (3)	C(11)-C(12)-C(14)	113.0 (8)	C(2)-C(3)-C(4)	108.3 (8)	C(2)-C(3)-C(8)	125.3 (8)
Cl(1')-Al(1)-C(11)	106.8 (3)	C(14)-C(12)-C(13)	108.8 (8)	C(3)-C(4)-C(5)	108.2 (7)	C(3)-C(4)-C(9)	125.7 (8)
C(1)-Al(1)-C(11)	143.7 (4)			C(4)-C(5)-C(1)	107.6 (7)	C(4)-C(5)-C(10)	127.1 (8)

Table VIII. Symmetry Representations, Eigenvalues, and a Partial Listing of Percent Orbital Characters for $[\text{CpAl}(\text{CH}_3)\text{Cl}]_2$

MO	eigenvalue, eV	major % orbital character	MO	eigenvalue, eV	major % orbital character
14b _u	2.53	Al 3s (19.8), Al 3p _y (25.8), Al 3p _z (31.9)	7b _g	-15.55	Cl 3p _x (51.8), Al 3p _x (24.7), Cp 1a ₂ (22.7)
13b _u	-12.56	Cl 3p _x (18.8), CH ₃ 2p _z (10.9), Cp 2b ₁ (62.4)	11b _u	-15.62	Cl 3p _x (30.0), CH ₃ 2p _z (14.7), Al 3p _z (11.5), Al 3p _y (12.1), Cp 2b ₁ (22.6)
9a _g	-12.80	Cl 3p _z (11.5), CH ₃ 2p _z (10.1), Al 3s (2.1), Cp 2b ₁ (67.7)	7a _g	-16.30	CH ₃ 2p _z (50.2), Al 3s (10.7), Al 3p _y (19.2)
9b _g	-12.86	Cl 3p _x (30.8), Cp 1a ₂ (66.4)	10b _u	-16.83	CH ₃ 2p _z (32.4), Cl 3p _x (28.4), Al 3s (17.1), Al 3p _y (11.1)
5a _u	-13.10	Cl 3p _z (45.2), Cp 1a ₂ (54.2)	5a _g	-20.15	Cp 1b ₁ (61.3), Al 3s (7.5)
12b _u	-13.30	Cl 3p _y (94.2)	8b _u	-20.21	Cp 1b ₁ (58.3), Al 3s (10.7)
8b _g	-13.44	Cl 3p _y (97.2)	1a _u	-28.61	Cl 3s (95.1), Al 3p _x (4.9)
4a _u	-14.31	Cl 3p _z (50.0), Al 3p _x (12.3), Cp 1a ₂ (36.6)	1a _g	-29.30	Cl 3s (85.8), Al 3p _x (9.1)
8a _g	-15.18	Cl 3p _z (66.4), Al 3p _z (10.8), Cp 2b ₁ (11.3)			

From an initial variational basis set of 80 valence atomic orbitals, 10 bonding and 6 nonbonding MOs remained important to the understanding of the interactions in the molecule. The relative energies of the Al and Cl atomic valence orbitals, the Cp valence MOs, the methyl group valence MOs, and the resulting MOs for the complex are presented in Figure 3. The orbital symmetry representations, eigenvalues, and a partial listing of the important percent orbital characters for these MOs and the LUMO 14b_u are listed in Table VIII. A full listing of percent orbital characters is given in Table S-11.

A brief description of the nature of the 10 bonding and 6 nonbonding MOs is warranted. The 1a_u and 1a_g MOs are mostly Cl 3s in character with smaller contributions from Al 3p_x and Al 3s and 3p_z, respectively. These MOs correspond to Al-Cl σ bonding interactions in the complex. The 5a_g and 8b_u MOs are mainly Cp 1b₁ in character. They are stabilized with respect to the free Cp⁻ ligand by interaction with the Al 3s, 3p_y, and 3p_z atomic orbitals, and these MOs correspond to Al-Cp σ bonding interactions. The 7a_g and 10b_u MOs are primarily CH₃ 2p_z and Cl 3p_x in character, and they provide additional contribution to the Al-Cl and Al-CH₃ σ interactions. The 4a_u MO contains Al 3p_x-Cl 3p_z and Al 3p_x-Cp 1a₂ interactions with the latter having π symmetry. The 8a_g MO is dominated by Al 3p_z-Cl 3p_z orbital interactions and Al 3p_z-Cp 2b₁ orbital interactions, and the Al-Cp 2b₁ overlaps have π symmetry. In a similar fashion 7b_g is dominated by Al 3p_x-Cl 3p_x σ overlap with a significant π symmetry overlap between the Al 3p_x AO and Cp 1a₂. The 11b_u MO is composed of Al 3p_y and 3p_z combinations with Cp 2b₁, Cl 3p_x, and CH₃ 2p_x orbitals, and the Cp 2b₁ interactions with Al 3p_y and 3p_z AOs have π symmetry. These four MOs, therefore, contain the Al-Cp π bonding and Al₂Cl₂ ring stabilization interactions which are most likely responsible

Figure 3. Molecular orbital diagram for $[\text{CpAl}(\text{CH}_3)\text{Cl}]_2$.

for the observed structures of 1 and 3.

The next six MOs including the HOMO 13b_u are nonbonding in character and for the most part they are localized on the CH₃⁻, Cp⁻, and Cl⁻ ligands. The LUMO

(61) For example, in C_{2h} symmetry the aluminum atomic orbitals transform as 3a_g, 3b_u, a_u, and b_g, the chlorine atomic orbitals transform as 2a_g, 2a_u, 2b_g, and 2b_u, the occupied Cp⁻ orbitals transform as 2a_g, b_g, a_u, and 2b_u, and the methyl carbon p_z orbitals transform as a_g and b_u. Consequently, the Al 3s, 3p_y, and 3p_z orbitals mix with Cp 1b₁ and 2b₁ orbitals to form MOs of a_g and b_u symmetry. The Al 3p_x and Cp 1a₂ orbitals mix to form an a_u and b_g MO set. The Al 3s, 3p_x, and 3p_z orbitals combine with the CH₃ 2p_z orbitals to give an a_g and b_u set, and the Al 3s, 3p_x, and 3p_z orbitals combine with Cl atom 3s, 3p_x, 3p_y, and 3p_z orbitals to form a_g, a_u, b_g, and b_u sets.

is predominately localized on the Al AOs and the Cp⁻ 1b₁ MO, and it is the antibonding counterpart of the Al-Cp σ bonding MO 8b_u. The separation between the HOMO and LUMO is large (~15 eV), and it is unlikely that the complex can be reduced by population of this orbital.

Overlap populations have been used to provide a measure of relative covalent bond orders,⁶² and an overlap population analysis for the Al AO and Cp⁻ MO interactions is informative.⁶³ The overlap population between the Al 3s, 3p_y, and 3p_z orbitals and the Cp 1b₁ MO total 0.134, and this corresponds to the Al-Cp σ bonding interactions. The Cp 1a₂-Al 3p_x overlap population 0.102 and the Cp 2b₁-Al 3s, 3p_y, and 3p_z overlap populations 0.101 represent the combined Al-Cp π symmetry overlaps. The overlap populations between the Al AOs and the Cp⁻ antibonding MOs 3b₁ and 2a₂ are negligible, and this is consistent with the absence of back-donation from the Al atom to the Cp π^* orbitals.⁶⁴ Last, the total Al-Cp overlap population 0.337 is similar to the Al-CH₃ total overlap in [CpAl(CH₃)Cl]₂, 0.314, and [(CH₃)₂AlCl]₂, 0.308. A summary of overlap populations appears in Table S-12.

The Al-Cp orbital overlap populations can be compared with the population in several transition-metal cyclopentadienyl complexes. In ferrocene, calculations have shown that the Cp-Fe σ overlap is small while the majority of the bonding interaction is derived from π -type overlaps between the metal d orbitals and Cp π and π^* orbitals.² In CpMn(CO)₃,⁴² it has been reported that there is a small σ symmetry overlap population, 0.022, between the totally symmetric a''₂ Cp MO and Mn atom. On the other hand, the Mn-Cp e''₁ π overlap population 0.304 and the Mn-Cp e''₂ σ^* overlap population 0.212 are large. On the basis of these comparisons, it is clear that the σ bonding component is more important in the aluminum complexes than in the transition-metal complexes. Similarly, the π^* contribution is far less important in the aluminum complexes. However, it is also apparent that the π bonding in the aluminum complexes is extremely important in determining the final structures, and it is this component which distinguishes these molecules from the normal η^1 - σ -bonded nonmetal-Cp compounds.

An examination of the two center overlap populations between the aluminum atoms and the individual ring

carbon atoms also is interesting. The Al-C(1) population 0.166 is largest, and the Al-C(2) and Al-C(5) populations are 0.097. As anticipated the Al-C(3) and Al-C(4) populations are very small, 0.005, and they are consistent with nonbonding interactions. The negligible overlap populations between the two aluminum atoms, -0.025, and the two chlorine atoms, -0.018, are also consistent with nonbonding interactions. A Mulliken charge distribution analysis reveals net charges of 0.342- for each Cp ring, 0.350- for each CH₃ group, 0.278- for each chlorine atom, and 0.941+ for each Al atom. Starting with the hypothetical separated groups, Al³⁺, CH₃⁻, Cp⁻, and Cl⁻, each CH₃ group donates 0.650 electrons, each Cp⁻ group donates 0.658 electrons, each Cl⁻ donates 0.723 electrons, and each Al atom ion accepts 2.059 electrons in forming the molecule. The high positive charge remaining on the aluminum atoms suggests that these atoms should be susceptible to nucleophilic attack and scission of the Al₂Cl₂ ring.

The spectroscopic and structural studies described here for **1** and **3** indicate that the pentamethylcyclopentadienyl ligand is able to interact in a novel fashion with [Al(R)Cl]₂ fragments. The theoretical analysis has provided a qualitative understanding of the electronic orbital interactions which contribute to determining the η^3 structures. The small distortions in the Cp* ring geometries and the ring slippage in **3** are not fully understood; however, it is likely that these distortions are derived from steric or nonbonded interactions. These results provide some interesting additional insights to the prior studies of alkylaluminum cyclopentadienyl complexes.

Acknowledgment. We wish to recognize NSF Grants CHE-780291 and MPS75-06111 which facilitated the purchases of the X-ray diffractometer and NMR data system. R.T.P. wishes to acknowledge partial support of this work by the UNM Research Allocations Committee. We also wish to thank Professors M. B. Hall, Texas A&M University, and D. L. Lichtenberger, University of Arizona, for valuable assistance with the MO calculations, and Professor R. Hoffmann, Cornell University, for bringing to our attention his study of haptotropic shifts across a Cp⁻ ring.

Registry No. 1, 72303-53-8; 2, 81457-43-4; 3, 81457-44-5; [(C-H₃)₂AlCl]₂, 14281-95-9; [(C₂H₅)₂AlCl]₂, 51466-48-9; [(i-C₄H₉)AlCl]₂, 51466-51-4; MgCp*₂, 74507-64-5; Cp*MgCl, 72303-54-9; Cp*Li, 51905-34-1.

Supplementary Material Available: Tables of observed and final calculated structure factors and tables of hydrogen atom positional parameters, thermal parameters, least-squares planes, MO orbital characters and eigenvalues, and overlap populations (31 pages). Ordering information is given on any current masthead page.

(62) Fenske, R. F.; Radke, D. D. *Inorg. Chem.* 1968, 7, 479.

(63) The overlap populations, expressed in terms of individual two center orbital populations, are available in the supplementary material, Table S-12.

(64) The Mulliken gross populations, in the transformed basis set, for the Cp ring MOs are as follows: 1b₁, 1.739; 1a₂, 1.815; 2b₁, 1.779; 3b₁, 0.005; 2a₂, 0.003. These populations are respectively 2.000, 2.000, 2.000, 0.000, and 0.000 in the free Cp⁻ ligand. The population shifts are consistent with σ donation from 1b₁ to the aluminum atom and π donation from 1a₂ and 2b₁ to the aluminum atom.